One hundred years of Moseley's law: An undergraduate experiment with relativistic effects

Tomas Soltis,[a] Lorcan M. Folan, and Waleed Eltareb
Department of Applied Physics, New York University Tandon School of Engineering, 6 MetroTech Center, Brooklyn, New York 11201

(Received 10 March 2016; accepted 16 February 2017)

As the centenary of H. G. H. Moseley's untimely passing approached, the authors undertook an evaluation of Moseley's work as the basis for an undergraduate laboratory experiment. Using a modern solid-state detector and low activity sources, characteristic *K* X-rays were excited and detected without the use of a vacuum chamber, from a selection of elemental metal foil samples from Ti to Er. The authors introduce first order relativistic corrections into the experimental analysis to obtain better fits for *K* X-ray energies that deviate substantially from Moseley's original law for elements beyond the first row transition metals. The experimental set up is described in detail, and the data and conclusions are readily reproducible by undergraduate students in the span of a couple of typical lab sessions.
[http://dx.doi.org/10.1119/1.4977793]

I. INTRODUCTION

In the spring of 1913, Hans Geiger and Ernest Marsden, working under the supervision of Ernest Rutherford, had just completed their large angle α particle scattering experiment. The results of Geiger and Marsden's experiment confirmed Rutherford's nuclear model of the atom and the idea that the α particle is the nucleus of a helium atom. In Rutherford's model of the atom nearly all of the mass of the atom was concentrated in a small central region with a positive charge C, and relative atomic mass of approximately $A = 2C/e$.[1] Rutherford believed that the success of this relation was in light of another trend, $\overline{\Delta A} \cong 2$, where $\overline{\Delta A}$ is the average change in the relative atomic mass between neighboring elements in the periodic table. Combining these two relations, he inferred that the change in charge ΔC between neighboring elements is approximately one electronic charge. Because α particles have a charge of $2e$ he took $C_{\mathrm{He}} = 2$, inferred that $C_{\mathrm{H}} = 1$, and deduced that the position number in the periodic table of elements, the atomic number Z, corresponded to the charge of the nucleus C.[2]

This line of argument provided support for the idea that the nuclear charge C controls the chemical properties of an element and not its mass A, and explained the inversions required for some elements in the periodic table where ordering by A did not correctly predict the chemical properties of the elements. An example of this was Co and Ni with atomic weights of 58.93 and 58.69, respectively, the order of which had to be reversed in the periodic table to account for the chemical properties. Furthermore, one would then expect the characteristic electromagnetic radiations to follow C as well. Atomic optical spectra show systematic variations that mostly correlated with chemical properties, e.g., alkali metals. Despite Rutherford's argument there was still discussion, which Niels Bohr gave considerable attention to, about whether the frequencies of characteristic X-rays should follow C or not. Bohr developed a model of the atom[3] that was based on the principle of quantized angular momentum. Using this model, Bohr was able to explain the optical spectrum of hydrogen as due to transitions between various quantized states, though it could not easily be extended to heavier elements.

At the end of 1913 and beginning of 1914, Henry Gwyn Jeffreys Moseley published two groundbreaking articles in the Philosophical Magazine.[4,5] There he described a simple linear law relating the square root of the frequency of characteristic X-rays emitted by an atom and the integer atomic number Z corresponding to that atom. Characteristic X-rays are emitted when an inner, core electron is removed from an atom forming a hole and another bound electron from a higher shell makes a transition to fill the hole; *K* X-rays are those emitted when an electron makes a transition from a shell with principal quantum number $n > 1$ to the innermost shell with $n = 1$. Greek subscripts have traditionally been used to distinguish transitions from different higher shells (e.g., K_α and K_β). To determine the frequency of the characteristic X-rays, Moseley used X-ray diffraction to disperse the X-rays onto a photographic plate. Knowing the diffraction angle θ, the interplanar spacing d, and the order of diffraction n, he could calculate the wavelength of incident radiation via Bragg's law $n\lambda = 2d\sin\theta$. Moseley obtained very good results using the first row transition metals plus calcium. Two lines were visible in each elemental X-ray spectrum, of which the α was the lower energy and the more intense.

In his analysis, Moseley introduced the quantity

$$Q = \sqrt{\frac{\nu}{\frac{3}{4}\nu_0}}, \tag{1}$$

where ν is the frequency of the measured X-ray, $\nu_0 = cR_\infty$ is the fundamental Rydberg frequency, c is the speed of light, and R_∞ is the traditional Rydberg constant. He found that Q is a quantity that increased uniformly, in approximately integer steps, from element to element. Being aware of Bohr's work on a model of the atom, Moseley argued that his work provided experimental verification that the angular momentum of an electron in a specific stationary state is the same for all the different elements.[4] Equation (1) can be derived from Bohr's theory on the assumption that the electron moved from stationary state 2 to 1, and the nuclear charge is reduced or screened by other electrons bound in the atom. The frequency of the principal characteristic radiation then becomes

$$\nu = \left(\frac{1}{1^2} - \frac{1}{2^2}\right)\frac{e^4 m_e}{8\epsilon_0^2 h^3} Q^2 = \frac{3}{4} cR_\infty (Z-\sigma)^2, \tag{2}$$

where σ is called the screening constant, e is the charge of the electron, m_e is the electron rest mass, ϵ_0 is the permittivity of free space, and h is Planck's constant. The numerical agreement between the constants ν_0 (which was obtained experimentally) and $e^4 m_0/8\epsilon_0^2 h^3$ was known to be very close at the time, while Bohr assumed them to the same for hydrogen.[3] Moseley found it quite remarkable that the experimental values and those calculated from a theory designed to explain the optical spectrum of hydrogen agreed so closely even though the frequencies differed by a factor of 2000.[4] It was only following publication of Moseley's work that the Bohr model was accepted as more generally correct and the nuclear charge in units of the electronic charge N became synonymous with the position number of an element in the periodic table Z (i.e., that $C/e = N = Z$). The mass-charge relation remained a mystery until the discovery of the neutron in 1932.

Moseley firmly established the order in which elements should be arranged in the periodic table by raising the atomic number Z to chemical preeminence over the atomic weight A. He confirmed that there exists in the atom a fundamental quantity that increases stepwise by one as we progress through the periodic table. This finalization of the periodic table left four gaps to be filled by elements yet to be discovered: technetium ($Z=43$), promethium ($Z=61$), hafnium ($Z=72$), and rhenium ($Z=75$). It also explained the need for three pairs of elemental neighbors to be switched from the mass ordering to reconcile with chemical periodicity: argon ($Z=18$) and potassium ($Z=19$), cobalt ($Z=27$) and nickel ($Z=28$), tellurium ($Z=52$) and iodine ($Z=53$).

Recently, high quality solid-state X-ray spectrometers have become available in compact form. Previous experiments suggested for undergraduate labs use radioactive sources with activities nearly 100 times larger than in our experiment,[6] and require vacuum systems or advanced equipment[7,8] that may not be available or appropriate for undergraduate students with little lab experience.[9] We also suggest an extension of the usual theoretical treatment to include relativistic effects unobservable with lower resolution spectrometers.[10] For this experiment, we were able to use a setup that does not require a vacuum system or high activity radioactive sources to excite the sample. This makes the experiment convenient to perform, while also minimizing the hazards due to radiation exposure.

II. THEORY

Moseley's law is quite accurate in predicting the energy of K X-rays for the first row transitions metals, but it starts to deviate substantially as one moves to higher Z elements. Equation (2) can be derived by solving Schrödinger's equation for an atomic system with an infinitely heavy nucleus and one electron. However, it does not take into account relativistic effects and electron spin, which are responsible for the fine structure of atomic electronic states.

Classic illustrations of relativistic effects, such as lifetime extension for cosmic ray muons, momentum and kinetic energy variations for charged particles in cyclotrons, etc., are difficult to include in an intermediate or advanced undergraduate laboratory course. However, the systematic variations of K X-ray energies are now readily observable and quantifiable, providing an additional and novel reason beyond historical importance to include a Moseley's Law experiment like this one in such a laboratory course.

The need to include relativistic effects can be understood from the virial theorem. Because the electromagnetic potential energy is proportional to the inverse of the distance between the bound particles, the virial theorem tells us that $2\langle T\rangle = -\langle V\rangle$. Here, $\langle T\rangle$ and $\langle V\rangle$ are the average kinetic and potential energies of the bound state, respectively. The energy of the bound state is equal to the sum of the potential and kinetic energies, $E = \langle T\rangle + \langle V\rangle$, so by the virial theorem, $E = -\langle T\rangle$. Since the energy of a characteristic X-ray is the difference in the energy between the initial state i and final state f, then $E_{\text{X-ray}} = E_i - E_f = \Delta\langle T\rangle$. The K X-ray energies at the end of the first row of transition elements approach 10 keV. This means that the kinetic energy of the electron also changes by 10 keV in the transition. However, 10 keV is about 2% of the 511-keV rest energy of the electron, and at this level it is generally accepted that relativistic effects must be accounted for in order to describe the bound system properly.

As discussed in a typical undergraduate quantum mechanics course, perturbation theory can be used to take these effects into account and correct the unperturbed Hamiltonian H_0. Overall there are three relativistic corrections that contribute to the fine structure of electron orbitals: the relativistic kinetic energy, the spin-orbit interaction, and the Darwin term.

Starting with the relativistic expression for kinetic energy and expanding in powers of the momentum p, we obtain

$$T = \frac{p^2}{2m_e} - \frac{p^4}{8m_e^3 c^2} + \cdots. \tag{3}$$

The first order kinetic energy correction is then

$$H_{\text{kinetic}} = -\frac{p^4}{8m_e^3 c^2}. \tag{4}$$

In the rest frame of the electron, the motion of the proton generates a current that in turn produces a magnetic field $\mathbf{B}$. This field creates a torque on the electron, tending to align its magnetic moment $\boldsymbol{\mu}$ along the direction of the field. The Hamiltonian for this interaction is $H = -\boldsymbol{\mu}\cdot\mathbf{B}$. Inserting appropriate expressions for the electron's magnetic moment, the magnetic field, and including a kinematic correction for Thomas precession, we obtain for the spin-orbit interaction

$$H_{\text{so}} = \frac{Ze^2}{8\pi\epsilon_0}\frac{1}{m_e^2 c^2 r^3}\mathbf{S}\cdot\mathbf{L}, \tag{5}$$

where r is the radial distance, $\mathbf{S}$ is the spin, and $\mathbf{L}$ is the orbital angular momentum of the electron. The third and final correction, called the Darwin term, is due to Zitterbewegung fluctuations in the electron position on the order of the Compton wavelength $\hbar/m_e c$, where $\hbar = h/2\pi$. As a result, the effective Coulomb potential is an average Coulomb potential over the characteristic distance $\hbar/m_e c$. The expression for this Darwin correction is[11,12]

$$H_{\text{Darwin}} = -\frac{1}{8}\frac{Ze^2\hbar^2}{m_e^2 c^2}\nabla^2\left(\frac{1}{r}\right). \tag{6}$$

The three corrections are of the same order of magnitude and when combined yield the first order relativistic correction for the binding energy of the electron

$$E(n,j,Z) = -hcR_\infty \left\{ \left(\frac{Z}{n}\right)^2 + \alpha^2 \left(\frac{Z}{n}\right)^4 \left[\left(\frac{n}{j+\frac{1}{2}}\right) - \frac{3}{4} \right] \right\}, \tag{7}$$

where $E(n,j,Z)$ is the energy of the electron, α is the fine structure constant, j is the total angular momentum, and n is the principal quantum number for the electron. The corrections have the effect of removing the degeneracy of the energy levels with the same n, and introducing a dependence on the total angular momentum quantum number j. For a particular transition, the photon energy is the difference between the initial and final state energies with principal quantum numbers n and m, and total angular momentum quantum numbers j and k, which yields

$$\begin{aligned} \Delta E_{nmjk} = E_{\text{X-ray}} = hcR_\infty \Bigg\{ & Z^2 \left(\frac{1}{n^2} - \frac{1}{m^2}\right) + \alpha^2 Z^4 \\ & \times \left[\left(\frac{1}{n^3\left(j+\frac{1}{2}\right)} - \frac{1}{m^3\left(k+\frac{1}{2}\right)} \right) \right. \\ & \left. - \frac{3}{4}\left(\frac{1}{n^4} - \frac{1}{m^4}\right) \right] \Bigg\}. \end{aligned} \tag{8}$$

This result is just Eq. (2), corrected for first-order relativistic effects and expressed as an energy E rather than a frequency ν.

While the previous equations are useful in calculating the binding energy of an atom with only a single electron, an extension must be made in order to account for the other electrons in a multi-electron atom. Gauss's law allowed Moseley to ignore the effect of outer electrons and assume that an electron in a multi-electron atom would move only under the influence of the net charge inside its orbital.[4] This means that Z in Eqs. (7) and (8) must be replaced with Q, the net effective nuclear charge the transitioning electron experiences. As before, the two are related by $Q = Z - \sigma$. Since each characteristic X-ray results from a transition from one energy level to another, we end up with expressions of the form

$$E_{K_{\alpha 1}} = hcR_\infty \left[\frac{3}{4}(Z - \sigma_{K_{\alpha 1}})^2 + \frac{15}{64}\alpha^2 (Z - \sigma_{K_{\alpha 1}})^4 \right] \tag{9}$$

for $K_{\alpha 1}$ X-rays, using $n=1 m=2, j=1/2 k=3/2$. Likewise for $K_{\alpha 2}$,

$$E_{K_{\alpha 2}} = hcR_\infty \left[\frac{3}{4}(Z - \sigma_{K_{\alpha 2}})^2 + \frac{11}{64}\alpha^2 (Z - \sigma_{K_{\alpha 2}})^4 \right], \tag{10}$$

using $n = 1\, m = 2, j = 1/2\, k = 1/2$. For $K_{\beta 1}$ and $K_{\beta 3}$, we obtain

$$E_{K_{\beta 1}} = hcR_\infty \left[\frac{8}{9}(Z - \sigma_{K_{\beta 1}})^2 + \frac{13}{54}\alpha^2 (Z - \sigma_{K_{\beta 1}})^4 \right] \tag{11}$$

and

$$E_{K_{\beta 3}} = hcR_\infty \left[\frac{8}{9}(Z - \sigma_{K_{\beta 3}})^2 + \frac{12}{54}\alpha^2 (Z - \sigma_{K_{\beta 3}})^4 \right]. \tag{12}$$

III. EXPERIMENT

For this experiment, we used a 3 mm × 3 mm CZT X- and γ-ray detector. CZT is a semiconductor being studied for use in compact and portable X- and γ-ray detectors.[13] Its characteristics are similar to those of the more frequently encountered CdTe,[14] and for a typical 1-mm thick detector crystal, the detection efficiency for X- and γ-rays exceeds 10% between about 2 and 200 keV.[15] Figure 1 shows the experimental set up. The detector was mounted on a plastic stand with slots to allow for insertion of samples. The stand was in turn covered in lead foil to reduce background signals, and also to shield the ^{241}Am excitation sources. Because CZT is piezoelectric, the detector setup was placed on a rubber mat to reduce vibration and noise pickup from the environment.

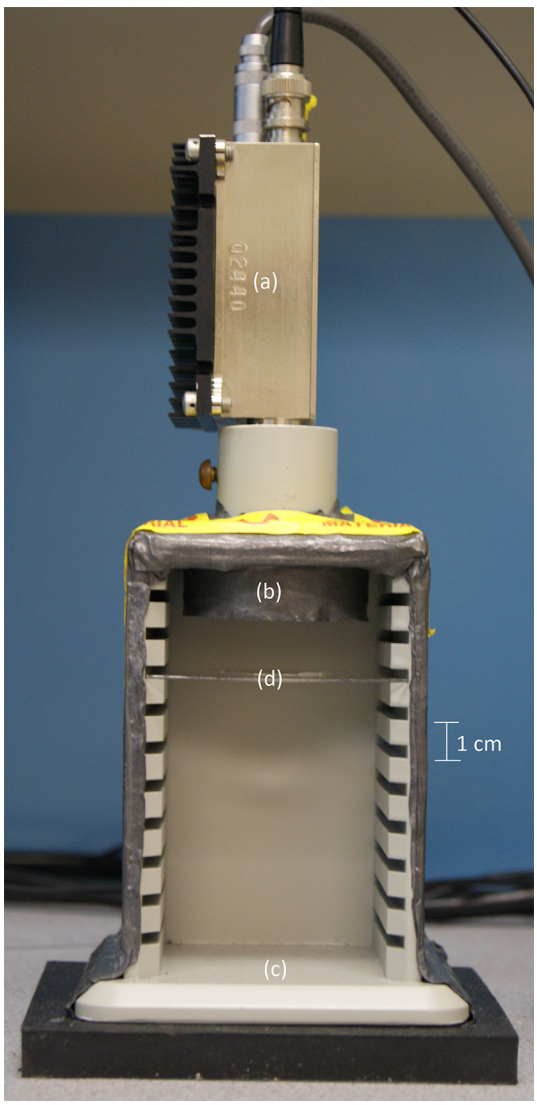

Fig. 1. The experimental setup including the detector (a), shielded source array (b), lead lined plastic stand (c), and plastic sample tray (d).

The detector has a built in thermoelectric cooler that keeps the CZT crystal at a temperature of approximately 230 K. Over time this causes the preamplifier housing to heat up, in turn making the thermoelectric cooler less effective at keeping the crystal cool. To counteract this, a heat sink was placed on one side of the detector and a small fan was pointed towards the unit. We found that this was sufficient to keep the unit operating stably.

Inside the shielded stand, we employed a source array composed of twelve 1-μCi ^{241}Am sources.[16] The dozen emitters were arranged on a section of the surface of a sphere of radius 20 mm with their convergence point being where the samples were placed for analysis. We chose to use air stable metal foils for their ready availability and ease of handling.[17] The source array is shown in Fig. 2. Americium-241 primarily emits 5.5 MeV α-particles and 59.54 keV γ-rays. The γ-rays are much more penetrating in air than the α-particles meaning that the primary source of excitation in the elemental samples was the γ rays. The 59.54 keV energy of the γ-rays thus puts an upper limit on the selection of elements whose K-shells can be excited. This limit in practice corresponds to about the K shell energy of Er ($Z = 68$).

The CZT detector was connected to a power supply and an amplifier that has a built in Rise Time Discriminator (RTD), which was in turn connected to a computer-based MCA spectrometer. The spectrometer was connected via USB to a computer where data was processed and displayed.

The 59.54 keV γ-ray from ^{241}Am, the 14.41 keV and 122.06 keV γ-rays from ^{57}Co, and the 81.00 keV γ-ray from ^{133}Ba were used to calibrate the instrument. A linear calibration was found to work best, as recommended by the manufacturer. The metal foil samples were placed on a thin plastic tray whose center was removed. We found that using a tray with a hole cut in it reduced the back-scatter from the ^{241}Am sources as compared to a tray with no hole. Six hundred-second live time spectra were recorded for the calibration as well as for all the metal foil samples except for Ti and V, where 1200-s live time spectra were recorded due to the low count rates.

X-ray spectra with reasonable signal-to-noise ratios were obtained and are shown for the available first row transition metals in Fig. 3. In this figure, we divided the number of counts in each channel for Ti and V by a factor of two in order to better illustrate the relative intensities observed as one progresses through the periodic table. The small sharp peak just below 60 keV was due to elastic back-scatter into the detector from the ^{241}Am sources, while the broader feature around 50 keV was due to inelastic scattering from the sample foils.

The K_α and K_β emissions were not resolved by the detector system for Ti and V. For these elements, we took the measured energy to be that of the K_α emission and we did not use equal (i.e., unresolved) values for the K_β energies in our analysis. The K_α and K_β lines become resolved for heavier elements, starting with Fe where the K_β line is seen as a shoulder. The K_β line begins to split into subcomponents at the element In, while the substructure of the K_α line becomes evident at the element Er. The peak positions were measured using the centroid feature provided by the MCA. A region of interest was defined around the peak of interest and an automated fit yielded the peak position and full width at half maximum (FWHM) estimates. Parallel measurements using the peak maximum positions gave similar but somewhat less reproducible results.

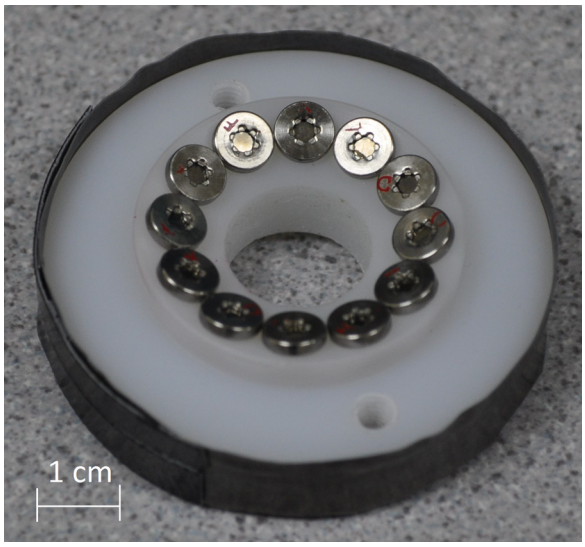

Fig. 2. The source array used to excite the metal foil samples. The exterior of the array is covered in lead foil to shield the sources.

IV. MOSELEY'S LAW

Following Moseley's original analysis,[4] Table I shows that the screened nuclear charge Q increases in approximately integer steps from element to element for the measured K_α X-ray energies, in lockstep with the atomic number Z. In calculating Q, we used the standard reference value for the Rydberg energy $hcR_\infty = 13.605$ eV.[18]

In Fig. 4, we plot the square root of the measured K_α energies against the atomic number Z and atomic weight A for the same group of first row transition metals. We see that the square root of K_α X-ray energies correlate much better with Z than A. The fact that Q increases uniformly with Z, and not A, offered striking proof that the atom contains a fundamental quantity that changes by unity from element to element—the electric charge of the nucleus.

We can perform a linear regression of the form $\sqrt{E} = mZ + b$ and combine it with

$$\sqrt{E_{K_\alpha}} = \sqrt{\frac{3}{4}hcR_\infty}\left(Z - \sigma^*_{K_\alpha}\right) \tag{13}$$

for K_α X-rays and

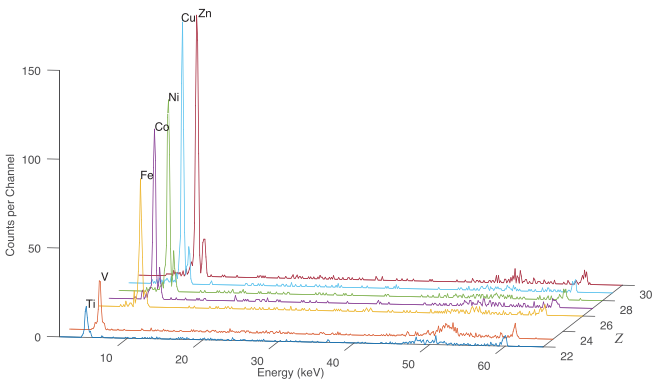

Fig. 3. Overlay of first row transition metals spectra.

Table I. Q values for K_α X-rays of the first row transition metals.

Element	Z	$Q_{K_\alpha} = [E/(\frac{3}{4}hcR_\infty)]^{1/2}$	σ_{K_α}
Ti	22	20.88	1.12
V	23	21.89	1.11
Fe	26	24.85	1.15
Co	27	25.88	1.12
Ni	28	26.90	1.10
Cu	29	27.88	1.12
Zn	30	28.95	1.05

$$\sqrt{E_{K_\beta}} = \sqrt{\frac{8}{9}hcR_\infty}\left(Z - \sigma^*_{K_\beta}\right) \tag{14}$$

for K_β X-rays. Doing so yields $hcR_\infty = (4/3)m^2$ for K_α, $(9/8)m^2$ for K_β, and the best fit screening constant $\sigma^* = -b/m$ for each. The results of this regression analysis are shown in the top section of Table II. We obtained a fairly accurate result for the Rydberg energy hcR_∞ using the K_α line. While the standard reference value is given as 13.6 eV, our result, using only the data from the first row transitions metals, was accurate to within 5%. While Moseley inferred a value of approximately 1 for $\sigma^*_{K_\alpha}$, our fitted value is higher at 1.25. This discrepancy can be explained in part by the larger fitted value of hcR_∞ we obtained as compared to the standard value. Since a larger Rydberg energy means more energetic X-rays, then σ has to increase as well to compensate. The larger Rydberg energy can be explained by the fact that for Ti and V, the K_α and K_β peaks were unresolved. Since the K_β X-rays are more energetic, the combined peak is shifted to a slightly higher energy.

When the same analysis is applied to all the elemental metal samples available where K X-rays could be excited $(22 \le Z \le 68)$, the calculated Rydberg energy and screening constant obtained are significantly larger, as shown in the lower section of Table II. In total 17 elemental samples were used in the experiment and a Moseley plot[5] of the full data set is provided in Fig. 5. Furthermore, when σ is calculated for each individual element, using the standard value for R_∞, the dependencies shown as Zeroth Order in Fig. 6 are obtained.

From these curves, as well as the results in Table II, it is clear that zeroth order Moseley's law is not sufficient to explain the variation of the characteristic X-ray energies for higher Z elements, thereby demonstrating the need for a correction.

Table II. Rydberg energy and screening constant from linear regression.

Samples	Line	hcR_∞ (eV)	σ^*
First row transitions metals	K_α	13.8 ± 0.1	1.25 ± 0.10
	K_β	12.9 ± 0.6	1.21 ± 0.65
All samples	K_α	14.9 ± 0.1	2.32 ± 0.17
	K_β	14.7 ± 0.2	3.08 ± 0.21

V. RELATIVISTIC CORRECTIONS

When fine structure cannot be resolved, as was the case in our experiment for all the samples except Gd and Er, a weighted mean of the fine structure components can be used to estimate the combined energy. The weights can be calculated using the intensity ratios for each sub-line, taken to be proportional to the multiplicity of the upper state $(2j+1)$, where j is the initial total angular momentum quantum number. This procedure was used to derive combined first-order K X-ray energy expressions. The K_{α_1} line is due to a transition from the $2p_{3/2}$ to the $1s_{1/2}$ state and the K_{α_2} from the $2p_{1/2}$ to the $1s_{1/2}$ state. A 2:1 ratio is obtained between K_{α_1} and K_{α_2} lines, yielding

$$E_{K_\alpha} = hcR_\infty\left[\frac{3}{4}(Z-\sigma_{K_\alpha})^2 + \frac{41}{192}\alpha^2(Z-\sigma_{K_\alpha})^4\right] \tag{15}$$

for the weighted mean energy. Similarly, we obtain

$$E_{K_\beta} = hcR_\infty\left[\frac{8}{9}(Z-\sigma_{K_\beta})^2 + \frac{19}{81}\alpha^2(Z-\sigma_{K_\beta})^4\right], \tag{16}$$

where K_β is also taken to be a 2 : 1 weighted mean between the $K_{\beta 1}$ and $K_{\beta 3}$ lines.

The first-order screening constant for each element can be calculated by plugging in the appropriate values for E and Z into Eqs. (15) and (16), and solving for $Q = Z - \sigma$. The zeroth-order screening constants for each element are obtained similarly from Eqs. (13) and (14). The value of Q for Eqs. (15) and (16) was calculated numerically using the `fzero()` function in MATLAB, which calculates the roots of functions. The overall trend can be seen in Fig. 6 where

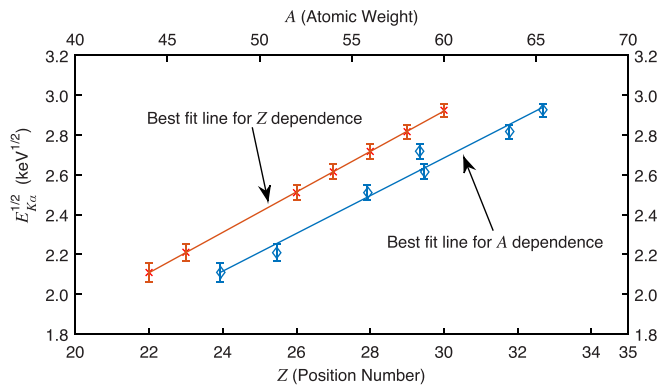

Fig. 4. Plot of the square root of the characteristic K_α X-ray energies versus Z and A. The energies of the K_α X-rays correlate much better with Z than A, confirming Moseley's conclusion.

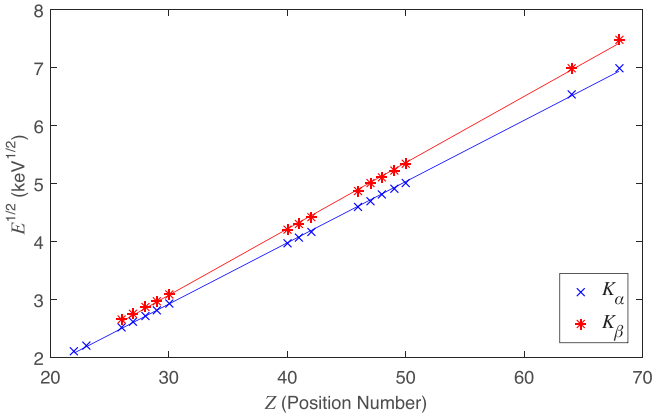

Fig. 5. Plot of the square root of K_α and K_β X-ray energies versus Z along with a best fit line for each transition.

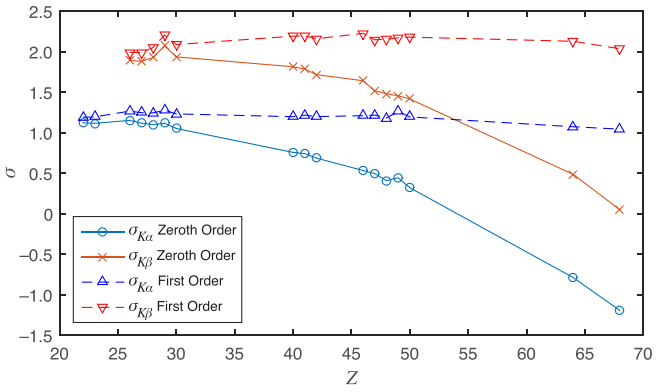

Fig. 6. Zeroth- and first-order screening constants for all samples. Applying a first-order correction to Moseley's law causes the screening constant to be more "constant," however, there is still some residual curvature towards high Z elements.

the zeroth order screening constant (original Moseley's law) exhibits a negative curvature. In fact, for some elements, σ becomes negative. This is an unrealistic result since it implies that a screened nucleus has a greater positive charge than a bare one which not possible if negative electrons are doing the screening. However, applying the first relativistic correction keeps the screening constant σ, as the name implies, much more "constant" throughout the larger range of elements, and eliminates the problem of negative σ's. Some slight curvature is still present, especially at Gd ($Z=64$) and Er ($Z=68$) where σ once again begins to decrease. This trend is expected to continue for even heavier elements.

In order to calculate the best fit value for the screening constant σ^*, we used the MATLAB `fit()` function to solve the nonlinear least squares problem. We once again used the standard value for R_∞ and let only σ^* vary. By varying the value of σ^*, the software is able to minimize the residual sum-of-squares value. The results of the analysis can be seen in Table III. Zeroth-order screening constants obtained in this way are highly inaccurate and imprecise because they take into account elements where the zeroth-order σ is close to zero or even negative as shown in Fig. 6. However, the first-order σ takes on more consistent values, which leads to a more precise best fit value σ^*. Performing a two parameter fit for σ^* and hcR using Eqs. (15) and (16), we obtain similar values for the best fit value of σ^* and much better values for hcR than with the zero-order expression. Although the number of K_β measurements is smaller (15 vs 17), a similar systematic improvement is obtained for both K series.

VI. CONCLUSION

We hope we have demonstrated that a Moseley's law experiment is an interesting and leading experiment for intermediate and advanced undergraduate students. Including relativistic corrections allows students to explore the effects of relativistic quantum mechanics on the structure of the atom and its X-ray emissions. The total cost of a similar apparatus, including the detector, pulse processing electronics, foil samples, excitation source, and plastic stand, but not including the host computer, would be about $8,750. Several previous Moseley's law experiments used strong radioactive sources, or specialized and expensive equipment. The cost of the apparatus described in Ref. 10, including the thin NaI(Tl) detector ($2,600), MCA and high voltage power supply ($3,100), source and samples ($750), but without a host computer is some $6,450. This apparatus allows observation of the variation of K X-ray energies between elements using weak radioactive sources, but not the observation and quantification of the relativistic effects discussed in this paper.

In this paper, we have included the first-order relativistic correction terms to Moseley's law, derived by applying perturbation theory to the non-relativistic Schrödinger equation. This procedure allows us to obtain a more accurate fit to experimental K_α and K_β X-ray energies. Furthermore, the first-order screening constant σ becomes much more constant even for heavy elements, unlike the zeroth order counterpart, which even becomes negative for two samples. This leads us to believe that a first-order correction term is an improved but not complete explanation of the K_α and K_β X-ray energies for our data set.

The screening constant does once again begin to exhibit negative curvature towards heavier elements such as Er and Gd, and this trend is expected to continue with heavier elements beyond our data set. This behavior leads us to believe that extra terms are needed to more accurately predict X-ray energies for those elements. In future work, we plan to use experimental X-ray transition energies such as those available from NIST[19] to explore higher-order terms as well as the fully relativistic Dirac expression. We will also explore additional corrections not included in the relativistic treatment, such as the finite nuclear mass correction to the Rydberg Constant, and attempt to extend the analysis to the L X-rays as well.

Table III. Screening constants obtained from MATLAB for the full data set.

Order	$\sigma^*_{K_\alpha}$	$\sigma^*_{K_\beta}$
Zeroth	0.17 ± 0.42	1.22 ± 0.39
First	1.16 ± 0.04	2.13 ± 0.04

ACKNOWLEDGMENTS

The authors would like to acknowledge the support of the NYU Tandon Summer Research Program, and the assistance of Christine Truong.

[a]Electronic mail: tomas.soltis@nyu.edu

[1]Sir Ernest Rutherford, "The structure of the atom," Philos. Mag. **27**(159), 488–498 (1914).
[2]J. L. Heilbron, *H. G. J. Moseley: The Life and Letters of an English Physicist, 1887–1915*, 1st ed. (University of California Press, Berkeley, CA, 1974), pp. 81–84.
[3]N. Bohr, "On the constitution of atoms and molecules," Philos. Mag. **26**(151), 1–25 (1913).
[4]H. G. J. Moseley, "The high-frequency spectra of the elements," Philos. Mag. **26**(156), 1024–1034 (1913).
[5]H. G. J. Moseley, "The high-frequency spectra of the elements Part II," Philos. Mag. **27**(160), 703–713 (1914).
[6]C. Hohenemser and I. M. Asher, "A simple apparatus for Moseley's law," Am. J. Phys. **36**(10), 882–885 (1968).
[7]C. W. S. Conover and John Dudek, "An undergraduate experiment on X-ray spectra and Moseley's law using a scanning electron microscope," Am. J. Phys. **64**(3), 335–338 (1996).
[8]P. J. Ouseph and K. H. Hoskins, "Moseley's law," Am. J. Phys. **50**(3), 276–277 (1982).
[9]W. Kiszenick and N. Wainfan, "X-ray emission and absorption exercise for introductory modern physics courses," Am. J. Phys. **42**(3), 161–166 (1974).

[10]S. B. Gudennavar, N. M. Badiger, S. R. Thontadarya, and B. Hanumaiahb, "Verification of Bohr's frequency condition and Moseley's law: An undergraduate laboratory experiment," Am. J. Phys. **71**, 822–825 (2003).
[11]David J. Griffiths, *Introduction to Quantum Mechanics*, 2nd ed. (Pearson Eduction India, New Delhi, India, 2007), pp. 279–287.
[12]John S. Townsend, *A Modern Approach to Quantum Mechanics*, 1st ed. (University Science Books, Sausalito, CA, 2000), pp. 322–331.
[13]Del Sordo, L. Abbene, E. Caroli, A. M. Mancini, A. Zappettini, and P. Ubertini, "Progress in the development of CdTe and CdZnTe semiconductor radiation detectors for astrophysical and medical applications," Sensors **9**, 3491–3526 (2009).
[14]Glenn F. Knoll, *Radiation Detection and Measurement*, 4th ed. (John Wiley & Sons, Hoboken, NJ, 2010), Chap. 13.
[15]The CZT detector used became available as the result of a research equipment upgrade. A 3 mm × 3 mm CdTe detector, with integrated power supplies and digital pulse processor, with characteristics comparable to the CZT detector and analog MCA used in these experiments, is commercially available from Amptek for $7,900.
[16]We made use of 241Am sources recycled from discarded smoke detectors. Cobalt-57 sources could be used instead to increase the range of measurable elements. The incremental cost would vary with the source configuration selected but individual unmounted 57Co sources are available commercially from suppliers such as Spectrum Techniques for about $100 each.
[17]A basic selection of six first-row transition metal foils (>99.9% pure) can be obtained from suppliers such as Alfa Aesar for about $150. The more extensive selection of 17 foils needed to fully reproduce our results would cost about $650. A plastic sample stand similar to the one used here is available from suppliers such as Spectrum Techniques for about $100.
[18]"CODATA recommended values of the fundamental physical constants: 2014," <http://arxiv.org/pdf/1507.07956v1.pdf>
[19]"X-ray transition energies database" <http://physics.nist.gov/PhysRefData/XrayTrans/Html/search.html>